Comparative Analysis of eVTOL, Drone, and Ground Transportation Systems for Emergency Delivery of Blood-Derived Medication

COMPARATIVE ANALYSIS OF EVTOL, DRONE AND GROUND TRANSPORTATION SYSTEMS FOR EMERGENCY DELIVERY OF BLOOD-DERIVED MEDICATION

Davide Angelini[1], Enrico Cestino[1], Daniela Cestino[2] & Francesco Cattel[2]

[1]Politecnico di Torino, Corso Duca degli Abruzzi, 24 - 10129 Torino (TO), Italy
[2]A.O.U. "Città della Salute e della Scienza di Torino", Corso Bramante, 38 - 10126 Torino (TO), Italy

Abstract

This study explores the viability of an innovative aerial delivery system for blood-derived medications in emergency scenarios by comparing electric Vertical Take-Off and Landing (eVTOL) aircraft and drones against the traditional ground transport methods. It also seeks to determine the most effective location for a delivery hub to enhance the efficiency of the transportation process.
Commencing with the development of a risk map, the study uses probability distribution functions and geospatial and demographic data from Meta and OpenStreetMap to identify sensitive areas for aerial overflight. The risk of catastrophic failure for eVTOLs was calculated using the Special Condition from EASA, and for ground delivery, regional statistics from the Piedmont area were utilized. The study then applies Dijkstra's algorithm to establish the safest and most efficient routes for the aircraft, benchmarking these against other routing methods. For ground transportation, the NetworkX software was used to find the best paths. Cost assessments for each transport mode were conducted for three different delivery urgencies, taking into account both fixed and variable costs. Comparing the transportation methods, the study finds that eVTOLs stand out for urgent and medium priority deliveries due to their adherence to safety standards and quick delivery times, while cars are recommended for routine deliveries because of their lower operational costs. The study concludes with the optimal placement of delivery hubs, suggesting that eVTOL hubs be located near hospitals with the highest demand for blood-related drugs, and ground transportation hubs on the outskirts of Turin to adapt to the area's road network.
Overall, the findings of this study offer new insights into the logistics of healthcare delivery, focusing on crucial aspects such as delivery speed, cost-efficiency, and safety.

Keywords: eVTOL, drone, urban air mobility, drug delivery, logistic

1. Introduction

In situations involving traumatic incidents such as road and skiing accidents, as well as during surgical procedures, the administration of blood-derived medications is essential. These medications are termed blood-derived because they are sourced from human blood donations rather than being synthetically produced. The unpredictable nature of accidents necessitates the use of these medications, complicating the application of traditional inventory management practices. Hospitals often maintain excess stock to ensure a minimum standard of care. However, sudden surges in demand compel hospitals to seek additional supplies from nearby facilities, thereby increasing the workload on hospital pharmacies and introducing risks associated with unplanned deliveries.
Currently, in the Piedmont area, medication deliveries are primarily conducted by special operators using cars, with rare instances of law enforcement agencies being involved (who primarily transport organs) . The lack of an adequate information network among hospital centers, warehouses, and manufacturing companies means that operators must manually contact various depots to locate the required medications.

Traditional delivery systems face challenges such as traffic congestion and road accessibility issues. Aerial transportation offers a potential solution to these challenges, although considerations of safety, reliability, and cost must be balanced. Notable use cases of drone deliveries in regions lacking proper transportation infrastructure highlight the potential of this method. For instance, drones have been used in Rwanda to transport blood and vaccines, and the company "Flirtey" has delivered medical supplies in Virginia (U.S.A.) [1]. Additionally, drones have been utilized for the rapid delivery of defibrillators [2]. The use of aerial transportation could reduce healthcare disparities in rural areas by employing the pickup method [3].

Several evaluations are underway to integrate aerial transportation into healthcare systems. For example, [4] presents a collection of use cases for drone deliveries. [5] provides a detailed analysis of the economic and environmental benefits in Southampton, United Kingdom.

However, urgent scenarios require critical evaluation of numerous elements, and the success of the mission is crucial. This complexity has slowed the adoption of aerial technologies in some cases [6]. Additionally, proper vertiports need to be strategically located to meet delivery needs. Researchers have investigated the optimal placement of these vertiports, ideally close to healthcare facilities [7]. Another challenge is path planning to minimize collision risks [8]. Given the expectation that drones will fly over densely populated areas, it is imperative to establish protocols for emergency landings to avoid harming individuals below [9].

This research aims to compare various strategies for transporting blood-derived medications in emergency conditions within densely populated contexts. Specifically, it will evaluate the current car-based delivery method against manned eVTOL (Vertical Take-Off and Landing aircraft) and drones. The case studies will focus on the 5th generation Wisk Cora for eVTOL and the Talon for drones. The evaluation will consider both the safety of flying over populated areas and cost-effectiveness. This research will conclude by identifying the optimal location for an emergency medication delivery hub.

2. Methods

First, we assess the safety of each transportation mode. For eVTOLs and drones, risk maps are utilized, incorporating various descent modes and population density to calculate the probability of catastrophic events. Each cell in the risk map contains an estimate of the likelihood that a catastrophic vehicle failure will result in a fatal impact with a person. These risk maps are generated using detailed probability density functions (PDFs) and statistical modeling (Section 2.4). Optimal paths are then determined using the A* algorithm (Section 2.5). For ground transportation, the NetworkX library in Python is employed to determine the shortest path (Section 2.6), leveraging statistical considerations such as accident rates and traffic data to assess the risk associated with different routes (Section 2.7).

Next, the results are applied to a dataset provided by the hospital pharmacy of the "Città della Salute e della Scienza" hospital in Turin, detailing real emergency deliveries in 2022.

Subsequently, the different transportation methods are compared using a merit index (Section 2.9). The merit index is a composite measure that accounts for various factors including safety, speed and cost. By standardizing these factors, the performance of eVTOLs, drones, and cars can be objectively evaluated across diverse scenarios.

Finally, the optimal location for a transportation hub is determined (Section 2.10). The hub serves as a central node for dispatching and receiving emergency supplies. Spatial analysis and optimization techniques are employed to identify a location that minimizes travel time and maximizes efficiency for all three transportation modes.

2.1 General Requirements of the Mission

Requirements play a critical role in the decision-making process for selecting the most appropriate transportation method based on the type of medication. The study starts from an analysis of the emergency drug deliveries made during the year 2022 engaging the hospital pharmacy of the "Città della Salute" hospital and other centers in Piedmont (sometimes in neighboring regions, such as Liguria for the "Gaslini" Institute or the U.S.L. of Val d'Aosta). The deliveries involved three classes of drugs:

- Class **A** drugs, i.e., with an **urgent** delivery requirement; these are life-saving drugs, such as blood products and/or antidotes, the administration of which must take place in the shortest possible time;
- Class **B** drugs, i.e., with **medium** delivery requirement; medicinal products whose administration is required in the shortest possible time but with an urgency requirement lower than class "A" fall into this category; it should be noted that in correspondence with lack of regional or national stockpiles or according to the conditions of patient admission to the emergency room, a class "B" drug may move to class "A"; for simplicity in the following analyses class "A" has been assigned to intrinsically life-saving medicinal products, thus disregarding special cases;
- Class **C** drugs and pharmaceuticals, i.e., with **routine** delivery requirement; these are products whose use is programmable in the following days, e.g. vaccines for the Covid-19 pandemic, sterile gauze, etc.

The dataset provided does not include normal pharmaceutical stock redistribution but corresponds to actual needs met by extraordinary deliveries for 2022. We go in details with the differences of mission profiles.
Urgent Delivery: In these scenarios, patients' lives depend on the prompt delivery of blood-derived medications. For instance, delivery is urgent if the payload is an antidote. The primary requirements for missions in this category include: highest priority on delivery time; flight safety as a secondary priority; acceptance of higher costs due to the emphasis on timeliness.
Medium Delivery: This profile balances delivery time and flight safety, with flight safety being important but secondary to the other factors.
Routine Delivery: For routine deliveries, flight safety during delivery is the highest priority, followed by cost control, and lastly, delivery time. This category is particularly suitable for scheduled deliveries of medications in non-critical situations.

2.2 Characteristics of the Payload

A blood-derived medication is defined as a drug produced "from human blood or plasma, sourced from voluntary donations, through industrial processing" (from "Blood-Derived Medications," Italian Medicines Agency [12]). When planning transportation, it is crucial to properly assess the risks involved, such as the effects of delivery delays or defects in refrigeration systems (from "Guide to the Preparation, Use, and Quality Assurance of Blood Components" [13]).
Given that these are life-saving medications, hospital facilities must always have a certain quantity available. They are stored in a lyophilized state and need to be dissolved (reconstituted) in saline solution before use. For instance, the medication "Kovaltry" must not be frozen and has a shelf life of 3 years if kept between 2℃ and 8℃, 12 months at room temperature (below 25℃), and only 3 hours from the time of preparation in water [14].
This section provides more details about the blood-derived medication Kovaltry, as it was used in the present research as a single case delivery.
Kovaltry [14] is a recombinant human coagulation factor VIII, used in patients with certain hemophilias. Specifically, it is used to stop bleeding and during surgical interventions. A single package contains both powder and solvent for reconstitution and subsequent intravenous infusion. Table 1 shows the storage times under different conditions.

Storage Conditions	Duration
In the refrigerator (2-8℃)	Up to 30 months
At room temperature (below 25℃)	12 months
After reconstitution	3 hours

Table 1 – Storage period of the medication "Kovaltry"

Under no circumstances should the medication be frozen. Figure 1.2 shows the contents of a Kovaltry 1000IU package. It can be sold individually or in batches of 30. In Section 6.2, the single package will be considered. Considering the contents, the weight of the package is estimated at 400g.

2.3 Area of Analysis

The evaluated area includes the city of Turin and a significant portion of the provinces of Piedmont. It is defined by the coordinates listed in Table 3.1. Figure 1 illustrates the larger rectangular area, as captured from Google Maps. Within this larger rectangle, there is a smaller rectangle specifically delineating the coordinates for Turin.

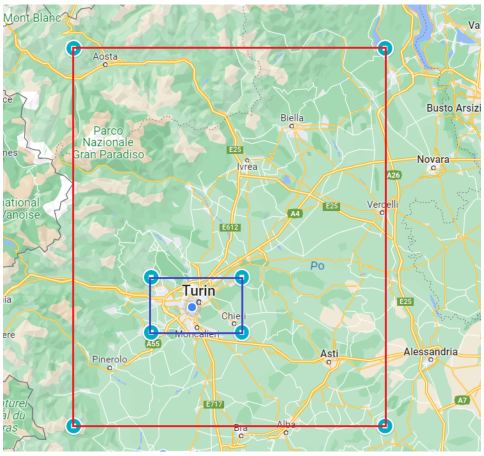

(a)

Overall area	
North [°]	45.7868
South [°]	44.7265
East [°]	8.4294
West [°]	7.1877
Turin area	
North [°]	45.1462
South [°]	44.9915
East [°]	7.8583
West [°]	7.4961

(b)

Figure 1 – Areas for the analysis; the red rectangle includes the overall area, the blue rectangle the city of Turin.

Figure 2 shows a satellite picture of the area considered, taken from Google Earth[1].

Figure 2 – Satellite picture of the area considered

2.4 Computation of the Risk Map

The risk map enables each cell to be associated with the overflight risk for a given area, making it a valuable tool for trajectory planning. It can be utilized as an input for path calculation algorithms to identify a minimum-risk trajectory. The primary reference for this work is Primatesta et al. [11], which details the computation of a risk map for drones. The formulation is represented by the following equation:

[1] Accessed: 13th June 2024

$$P_{casualty} = P_{event} \cdot P_{impact} \cdot P_{fatality} \tag{1}$$

To elaborate:

- P_{event} represents the probability of catastrophic damage to the aircraft;
- P_{impact} represents the probability that, as a consequence of the catastrophic damage, the aircraft impacts a person on the ground during its fall;
- $P_{fatality}$ represents the probability that such an impact is fatal for the person.

Thus, the value of $P_{casualty}$ indicates the probability that catastrophic damage to the aircraft results in a fatal impact on a person below. This tool allows for the determination of the safest route for an aircraft.

2.4.1 Determination of P_{event}

The P_{event} represents the probability that catastrophic damage occurs to the aircraft. Its value has been determined according to the study of regulations for drones and eVTOLs, and following statistical considerations.
The consideration of P_{event} for eVTOL aircraft involves a comprehensive regulatory framework and a meticulous approach to ensure safety and reliability. The European Aviation Safety Agency (EASA) has issued specific guidelines to address the unique characteristics of VTOL aircraft. On July 2, 2019, EASA introduced the "Special Condition for small-category VTOL aircraft" [15], recognizing the need for a distinct regulatory framework, as VTOLs do not fit within existing categories such as CS-23 (for light aircraft under 5,700 kg maximum take-off weight) or CS-27 (for helicopters up to 3,175 kg maximum take-off weight).
To determine the minimum acceptable risk level of catastrophic failures for VTOLs, a comparison with existing standards for helicopters (CS-27) and large civil aircraft (CS-25) is necessary.
The CS-27 [16] regulation categorizes helicopters based on their ability to continue safe flight following an engine failure, distinguishing between Category A (requiring an emergency landing) and Category B (capable of continuing flight). Further classification is based on maximum take-off weight (MTOW) and the number of occupants.
According to CS-25 [17], the permitted probability of failure depends on the type of damage and its consequences. Specifically, for lethal damage to part of the crew or passengers, the failure probability limit is 10^{-7}, while for catastrophic damage, it is 10^{-9}.
For the specific case of the Wisk Cora VTOL, which falls into the "Basic" category for 2 to 6 passengers, the regulatory framework suggests a catastrophic failure probability of 10^{-8} per flight hour. Therefore, the chosen P_{event} is $10^{-8}\,h^{-1}$.
For drones, due to different design requirements, $P_{event} = 10^{-2}\,h^{-1}$ has been used in accordance with previous analysis by Primatesta et al. [11].

2.4.2 Determination of P_{impact}

The P_{impact} represents the probability of an aircraft impacting a person during its fall. Within the context of a grid with dimensions $N1 \times N2$, it can be determined using the following equation:

$$P_{impact}(i,j) = \rho(i,j)A_{exp} \tag{2}$$

Here, $\rho(i,j)$ denotes the population density at cell (i,j), and A_{exp} represents the area of a person exposed to the crash.
Population density is a crucial factor for flight safety. In this study, we utilized the open-source dataset from Meta [18], which provides a map of Italy with a 30-meter cell grid, each cell containing population density data. Primatesta et al. [11] used a similar dataset based on census data [19]. However, we opted for the Meta dataset due to its more recent updates and higher resolution. The map is adjusted according to the dimensions of the desired grid ($N1 \times N2$). Figure 3 shows the population density of Turin for the area specified in Table 1, according to the chosen grid. The Po river is identifiable at the top left of each image.

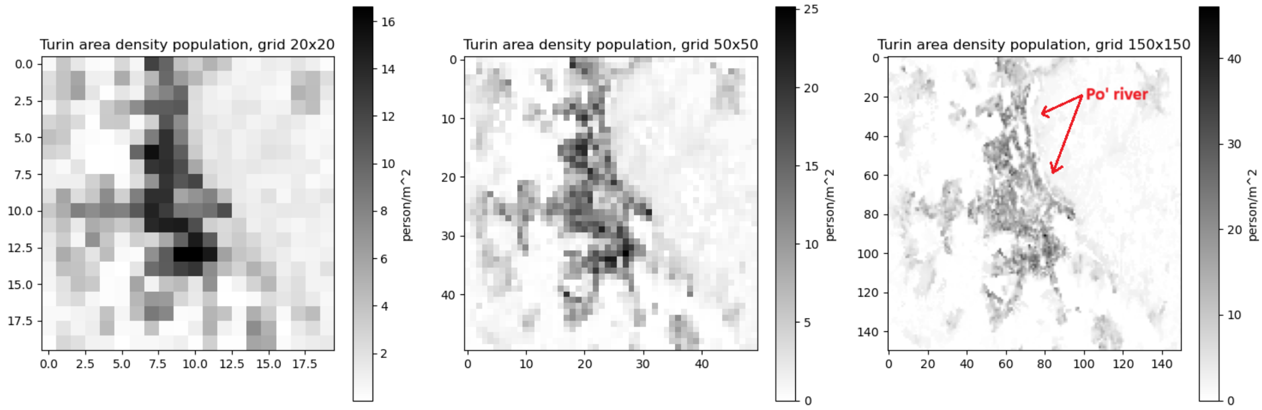

Figure 3 – Population density map based on the adopted grid precision.

A_{exp} represents the area of a person's body potentially subject to impact by space reentry objects, as referenced in a note from the airworthiness organization Federal Aviation Administration (FAA) [20]. The body is approximated as a cylinder with a radius r_p = 30 cm and a height h_p = 180 cm. The value of A_{exp} is given by:

$$A_{exp} = 2(r_p + r_{VTOL}) \cdot \frac{h}{\tan(\theta)} + \pi(r_{VTOL} + r_p)^2 \tag{3}$$

where θ is the angle of impact with the ground. In (3), the parameters are constant except for θ, which depends on the way the aircraft hits the ground. It is estimated from the ground impact velocity components:

$$\theta = arctan(\frac{|V_y|}{|V_x|}) \tag{4}$$

The flight conditions are detailed in Table 2. In practice, it is reasonable to assume that information such as the initial position or initial velocity may not be precisely known; therefore, a probabilistic approach using a statistical normal distribution is employed. Table 2 presents the values for the Wisk Cora used in the example calculation, sourced from [21] for eVTOL and [11] for drones. Values marked with "*" indicate assumed values. The exact value of the speed depends on the mission

	Wisk Cora (eVTOL)	*Talon* (drone)
Flight altitude* [m] according to normal distribution	$\mu_h = 700$ $\sigma_w = 70$	$\mu_h = 50$ $\sigma_w = 5$
Mass [Kg]	1224	1.4
Wing surface [m^2]	10	0.02
Average wind speed* [m/s] according to normal distribution	$\mu_w = 2.78$ $\sigma_w = 0.55$	$\mu_w = 2.78$ $\sigma_w = 0.55$
Air density [kg/m^3]	1.225	1.225
Maximum speed* [m/s]	50	5

Table 2 – Data for *Wisk Cora* and *Talon* for ballistic descent.

profile (Section 2.1). For urgent missions, it is expected that the speed will be maximized to ensure prompt delivery, therefore the sum of V_x and V_y is equal to the maximum speed of the aircrafts. Conversely, for less urgent missions, the need to reach the destination as quickly as possible is less critical. For example, in Medium priority we set $\mu_{V_x} = 56\% V_{max}$ and μ_{V_y} accordingly so that the overal velocity μ_V is $57\% V_{max}$. Both impact points and impact velocities depend on how the aircraft falls. Two falling methods are considered: *ballistic descent* and *uncontrolled glide*.

Ballistic descent refers to the uncontrolled fall of the aircraft, influenced solely by gravity and aerodynamic drag. The primary reference for this method is the work of La-Cour Harbo [22]. The algorithm implemented iis detailed in [23].

	Urgent	Medium	Routine
μ_{V_x}	$70\% V_{max}$	56% V_{max}	49% V_{max}
σ_{V_x}	10% μ_{V_x}	10% μ_{V_x}	10% μ_{V_x}
μ_{V_y}	$\sqrt{V_{max}^2 - \mu_{V_x}^2}$	$\sqrt{(80\% V_{max})^2 - \mu_{V_x}^2}$	$\sqrt{(70\% V_{max})^2 - \mu_{V_x}^2}$
σ_{V_y}	10% μ_{V_y}	10% μ_{V_y}	10% μ_{V_y}

Table 3 – Speed for the analysis

In the *Uncontrolled Glide* descent mode, the pilot loses control of the aircraft, which then descends at a glide angle determined by its geometry and aerodynamic conditions. For fixed-wing drones, this occurs in the event of a loss of engine power or control surface efficiency; for single or multi-rotor drones, the glide angle is governed by the autopilot.
The horizontal distance traveled is given by the glide ratio multiplied by the descent height:

$$dist(h) = \gamma \cdot h \tag{5}$$

where γ is the glide ratio from [11].
Using a probabilistic approach, the initial velocity values (in the X and Y directions), height, and wind speed are modeled with a normal distribution. The assumed values are the same as those in the ballistic descent, with the only difference being the definition of the PDF, which includes the value from equation 5 and the time of impact according to the following equation [11]:

$$t_{im} = \frac{V_{yi} + \sqrt{V_{yi}^2 + 2 \cdot 9.81\,\mathrm{m/s^2} \cdot h}}{9.81\,\mathrm{m/s^2}} \tag{6}$$

At the end of the computation, the overall P_{impact} is given by:

$$P_{impact} = P_{impact_{ballisticDescent}} + P_{impact_{uncontrolledGlide}} \tag{7}$$

2.4.3 Determination of $P_{fatality}$

The *fatality probability* estimates the likelihood that an impact with a person would be fatal. The most influential factors are the terminal impact energy and the sheltering provided by objects such as rooftops, trees, etc. Various approaches can be employed to estimate this probability. We take into consideration the methodologies from Dalamagkidis et al. [24] and Primatesta et al. [11] regarding the choice of the sheltering factor.
Dalamagkidis et al. [24] adopt the sheltering factor to avoid overestimating the risk of overflight, considering that urban elements such as buildings and trees can mitigate severe impacts. The author defines $34J$ as the impact energy required to cause harm to a person (based on the Range Safety Group [25]). The fatality probability is formulated as follows:

$$P_{fatality} = \frac{1}{1 + \sqrt{\frac{\alpha}{\beta}} \left[\frac{\beta}{E_{imp}}\right]^{\frac{1}{4p_s}}} \tag{8}$$

where p_s is the sheltering parameter, which can take a value in the range $p_s \in (0, 1]$. Here, $\beta = 34J$, α represents the impact energy required for a fatality probability of 1 with $p_s = 0.5$, and E_{imp} is the impact energy defined as $E_{imp} = 0.5 \cdot M \cdot V^2$. The author suggests using an average value of $p_s = 0.5$, considering that with $p_s = 1$, there is better coverage and lower risk for the same kinetic impact energy.
On the other hand, Primatesta et al. [11] formulates $P_{fatality}$ to account for different types of cover:

$$P_{fatality} = \frac{1-k}{1 - 2k + \sqrt{\frac{\alpha}{\beta}} \left[\frac{\beta}{E_{imp}}\right]^{\frac{3}{p_s}}} \tag{9}$$

where $k = \min\left(1, \left(\frac{\beta}{E_{imp}}\right)^{\frac{3}{p_s}}\right)$. In this approach, $p_s \in (0, \infty)$. However, since for $p_s > 10$, the probability approaches a machine-like value close to 0, they suggest to use $p_s = 10$ for industrial building cover, $p_s = 7.5$ for civilian buildings, and $p_s = 2.5$ for trees. In practical implementation, they do not make this distinction and use $p_s = 7.5$ where there are buildings.

Between the two treatments for $P_{fatality}$, we follow the approach from Dalamagkidis et al. [24] because it is more suitable for both drone and eVTOL cases.

For constructing the shelter map, the open-source database from OpenStreetMap was used[2]. Buildings are saved with a series of characteristics, including the coordinates of the perimeter points.
To map the buildings in an area of interest, a Python code was developed to identify all buildings with the tag *building = True* in the area of the selected coordinates in Table 1. The picture 4 shows an example fo buildings for the area of Turin.

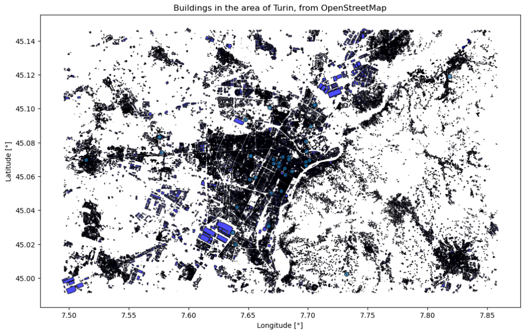

Figure 4 – Buildings with tag *building = True* in the area of *Turin, Italy* from OpenStreetMap.

The choice of the sheltering factor depends on the number of buildings protecting inhabitants in each cell. Some cells may have more buildings, while others have fewer. Then, we calculate the average number of buildings per cell, denoted as $N_{average}$. If a cell has a number of buildings N greater than the average, the chosen value is $p_s = 0.5$ in (8) following Dalamagkidis et al. [24]. Otherwise, for $N < N_{average}$, the value is set on $p_s = 0$.

The overall algorithm for the $P_{fatality}$ is similar to what it has been described in 2.4.2 for both *ballistic descent* and *uncontrolled glide*, the difference is that we employ the equation (8).

2.5 Determination of Optimal Path in Aerial Transportation

The trajectory calculation was implemented by starting with a simple problem and gradually adding variables to increase complexity. Initially, the trajectory of absolute minimum risk was determined using the Dijkstra algorithm [26], applied to the previously processed risk map.
Dijkstra's algorithm [26] is a static method that calculates the path of minimum risk on a graph where each movement is associated to a risk level. In the context of a map, each cell is connected to its adjacent ones (horizontally and vertically, but not diagonally). The path found has the global minimum risk; however, the resulting path can sometimes be convoluted. Considering that an eVTOL vehicle is less responsive in maneuvers compared to a drone, the analysis then transitioned to the A* algorithm [27] to account for more realistic and straighter trajectories.
The A* algorithm [27] finds the path of least risk based on a heuristic function. This algorithm is better suited to optimization problems because, unlike Dijkstra's algorithm, which only considers the predetermined risk value associated with each map cell, A* also analyzes the distance between the current point and the destination. Consequently, the trajectories found by A* are more uniform. Choosing an appropriate heuristic function is crucial. An overly optimistic heuristic (underestimating

[2]Open Street Map homepage

the cost) might lead to seemingly shorter paths that actually have higher risk. In our research we choose to use the Manhattan heuristic.

2.6 Determination of optimal path in Ground Transportation

While drones and eVTOL can virtually explore every point on a map, ground transportation is inherently linked to the presence of road networks. Consequently, the path of minimum risk coincides with the shortest route, as a longer journey increases the risk of accidents. To determine the car route, we used the open-source library *OpenStreetMap* to generate a graph with all the roads of considered area. This graph already contains information about the direction of travel, enabling us to find the most realistic path. The shortest car route is then obtained using the Python library *NetworkX*[3], which employs the Dijkstra's algorithm.

2.7 Evaluation of risk for Ground Transportation

To assess the risk of car transportation, accident statistics are taken into account. The concept of P_{event}, which measures catastrophic failure in aircraft, requires an analogous indicator for automobiles. An analysis was conducted based on the document "L'Incidentalità Stradale sulla Rete Viaria Principale" (Road Accidents on the Main Road Network) produced by the "Automobil Club d'Italia" on behalf of the Italian Ministry of Infrastructure and Transport ([29]). As an equivalent to P_{event}, the accident rate per 100 km is considered. According to data for the Piedmont region in 2017, there was an average of 2.64 fatal accidents per $100km^2$. Therefore, the safety of a route is evaluated by multiplying the route's length by the determined coefficient, resulting in a dimensionless number comparable to the aeronautical P_{event}:

$$P_{event_{ground}} = \frac{0.00264}{\text{km}} \tag{10}$$

2.8 Evaluation of costs

Evaluating the cost of transportation is a crucial parameter in enhancing the efficiency of the delivery system. It also provides a concrete measure of the feasibility of the results achieved.
This section presents basic models to estimate the costs associated with eVTOL, drone, and car deliveries.

2.8.1 Aircraft Cost Model

As a first approximation, the operational cost of eVTOL or drone travel was determined by considering the following factors: the salary of the pilot if the aircraft is manned; the cost of recharging the battery at the end of the route; and infrastructure operating costs.
The assumption is that the aircraft travels at a constant speed equal to the mission speed, as shown previously in Table 3. Thus, the flight time can be estimated as $t_{flight} = \frac{l_{path}}{V}$. Other hypothesis are: a pilot's working time is 35 hours per week[4]; an average month consists of 4 weeks; a gross monthly salary of €8.000,00. Therefore, the cost per hour results in the following:

$$c_{pilot} = \frac{monthly\,salary}{weekly\,working\,hours} = \frac{8000}{35h \cdot 4} = 57.14/h \tag{11}$$

For the charging battery cost, the average power consumption is estimated as the battery capacity divided by the aircraft range:

$$c_{power_{average}} = \frac{Battery\,capacity}{Aircraft\,range} \tag{12}$$

Therefore, by indicating with P_{charge} the price of charge (assumed as €0.45/kW), the cost of chage is the following:

$$c_{charge} = l_{path} \cdot c_{power_{average}} \cdot P_{charge} \tag{13}$$

[3]NetworkX Website
[4]estimate taken from Urbe Aero

Finally, an estimate of the operational cost of eVTOL is provided. Duffy et al. [31] address the issue of VTOL costs and suggest methods to reduce them based on engine type. The Wisk Cora falls into the "stopped rotor" category described in the paper because it has 12 vertical propellers for takeoff and additional horizontal propellers for cruising.
Using data from Aircraft Cost Calculator [30], we obtain the costs associated with daily maintenance, battery changes, and other factors (excluding fuel). As a conclusion, for the Wisk Cora the operating cost is $c_{operation} = \$197/h$.

The length of the path is the number of cell per the diagonal of them, according to the dimension of the grid chose $N1 \times N2$. The overall cost is the following:

$$c_{delivery} = c_{pilot} + c_{charge} + c_{operation} \tag{14}$$

2.8.2 Ground Transportation Cost Model

An average speed of 50 km/h is assumed. Although higher speeds may be achievable under emergency conditions, it is necessary to account for the influence of small roads and traffic, as 50 km/h is the speed limit in most Italian cities. The duration of the delivery is estimated as:

$$t_{delivery_{ground}} = \frac{l_{path}}{V_{ground}} \tag{15}$$

By considering fuel cost as €1.90/l, gross salary of the driver of €30.000,00 per year (according to exstimation of A.O.U. Città della Salute hospital) and a consumption[5] of 20.8l/km, we obtain:

$$\begin{aligned} c_{ground} &= c_{driver} + c_{fuel} = \\ &= \frac{€30.000}{12*40*4} \cdot t_{delivery_{ground}} + €2/l \cdot l_{path} * \frac{1000}{20.8km/l} \end{aligned} \tag{16}$$

2.9 Merit index

A merit index was constructed to compare different means of transportation, providing a quantitative measure of their suitability for a given mission. The reference work is by Cestino and Romeo [32]. Depending on the specific mission, the definition of the weights varies, rewarding certain characteristics of the transportation means.
First, thresholds are defined that the medium must meet. Specifically, the following criteria are established:

- **Payload condition**: The payload must be less than the maximum payload capacity for the aircraft or transportation medium.
- **Path length condition**: The path length must be within the maximum range for the aircraft or transportation medium.
- **Safety condition**: The risk associated with the route must be below a set limit.

If the transportation means meets the required thresholds, the merit index is calculated as follows:

$$I = \frac{\sum_i W_i \frac{(I_i - I_{min/max})^2}{(I_{max} - I_{min})^2}}{\sum_i W_i} \tag{17}$$

where I_i represents the magnitude to be evaluated for that particular means i, $I_{max/min}$ is the maximum or minimum of the magnitude under consideration among the means judged suitable, and W_i is the weight assigned to the measure under consideration (ranging from 0 to 10).
The three quantities considered in the following analysis are: Transportation **cost**; Overall **safety** of transportation; Delivery **time** (Table 4). The values of the W_i weights change depending on the

[5] From Motor1, accessed 11th June 2024

specific mission. As specified in the introduction (Section 2.1), three mission profiles are defined: **urgent**, **medium**, and **routine**. Table 4 shows the weights adopted for the first mission profile, related to blood-derived drugs. As can be seen, the highest importance is given to time since it is critical to deliver the drug as quickly as possible. Conversely, the lowest weight is given to the cost of delivery, while safety takes an intermediate value. It is important to note that **the merit index is calculated only when the above thresholds are met**. Assigning a lower value to safety does not imply risking the failure of the delivery mission because the minimum safety requirement must always be met. Rather, it is a matter of prioritizing one capability of the transportation means over another, in this case, delivery time.
In the case of the *medium* mission (Table 4), the security of delivery takes on more importance, although it does not reach the maximum value of 10; there is a balance between security of delivery and cost. For the *routine* delivery, security has the highest weight, followed by delivery cost, while time has the lowest value.

		Mission priority		
	Meaning	*Urgent*	*Medium*	*Routine*
W_{cost}	Transportation **cost**	2	4	8
W_{safety}	Overall **safety** of transportation	5	8	10
W_{time}	Delivery **time**	10	6	4

Table 4 – Weights for different mission profiles

The minimum threshold to be exceeded for the calculation of the risk map is $P_{casualty_{global}} > 10^{-6}$, obtained by summing the risk values of each cell in the map, as stated in [11].
For car delivery, no safety threshold was set. Instead, the value of 0.264 failures/km determined in Section 2.7 was considered when evaluating the merit index.

2.10 Determination of Optimal Hub Position

In the actual analysis, movements are discrete since it is only possible to move to adjacent cells. Additionally, the number of hospitals in the considered region is limited. Consequently, it is not computationally intensive to verify whether each cell in the map can serve as a hub position, thus complex algorithms are not required.
In this analysis, we follow a simple algorithm in Figure 5.

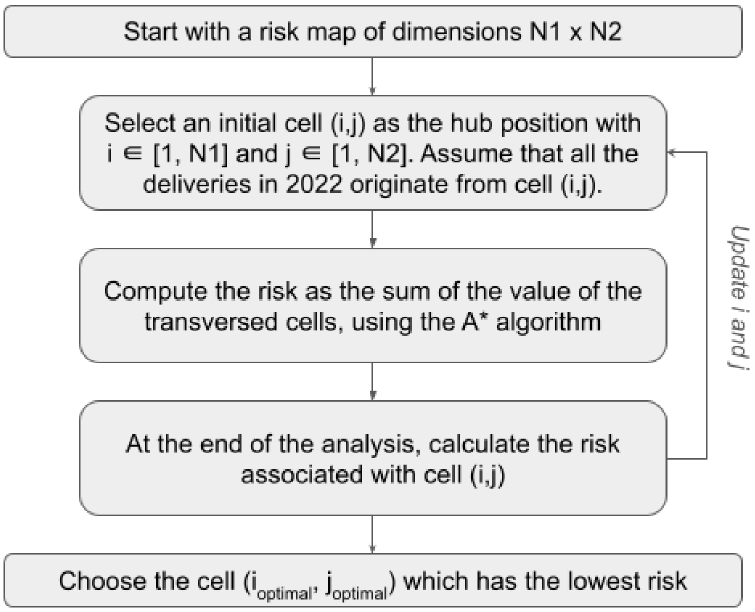

Figure 5 – Algorithm to determine the hub position

For the evaluation of the hub for cars, the approach is the same. However, since we do not have a risk map, the only difference is that we compute the shortest paths using NetworkX, determine the distance of these paths, and use Equation 10 to calculate the associated risk. In our model, the longer the path, the greater the risk; therefore, the safest path corresponds to the shortest one.

3. Results

First of all, general maps are build with resolution N1xN2 = 400x400. The dimension of a single cell are 382m (in direction east-west) and 451m (in direction north-south). In Figure 6 the results for Risk Map are displayed. We can recognize the shape of urban development in Figure 2.

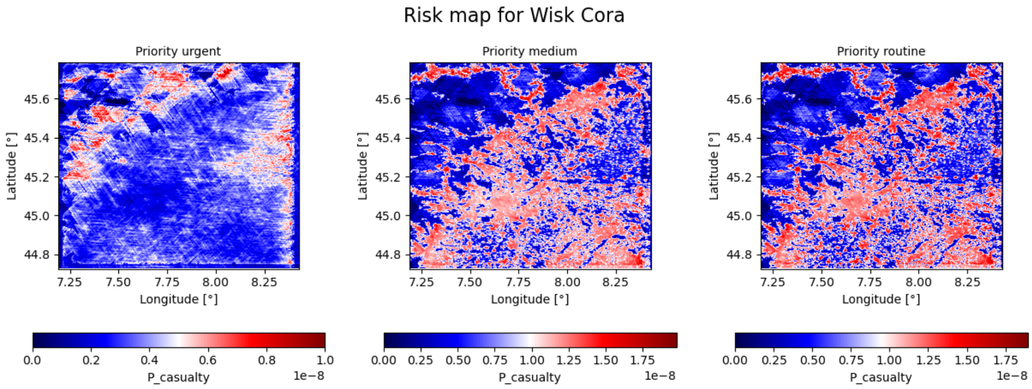

(a)

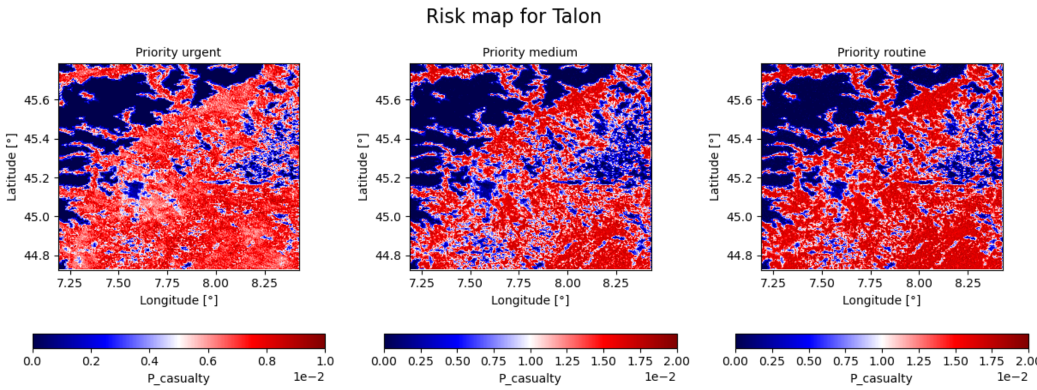

(b)

Figure 6 – Results of risk map; (a) for eVTOL, (b) for drone.

Figure 7 illustrates the needs of various hospitals in the Piedmont and Turin areas in 2022. The larger the dot, the greater the demand for urgent medicines. As shown, the hospitals with the highest demand for medicines were the "Mauriziano" and "Città della Salute".

We first test the implementation with a single delivery example of the medicine Kovaltry, classified as an urgent priority, in a round trip from the starting point at "Città della Salute" Hospital (45.0671, 7.6284) to the endpoint at "Martini" Hospital (45.0417, 7.6742). The most suitable means of transportation is the eVTOL. The merit index results are shown in Table 5. The result for the drone is 0 because it does not meet the payload threshold, thus its value defaults to 0. Additionally, the risk threshold is not met, with the overall safety being $0.29h^{-1}$. Figure 8 shows the paths computed for both eVTOL and car.

The same results can be extended to all the dataset of deliveries in 2022. Tables 6, 7 and 8 show how many times the threshold of Safety, Payload and Range respectively were respected for aircrafts (round trips); as stated in section 2.9, for cars no thresholds have been applied, however the risk

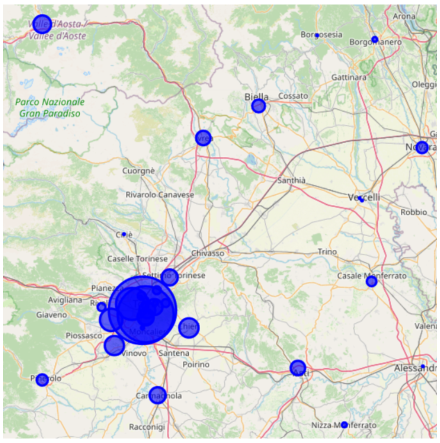

(a)

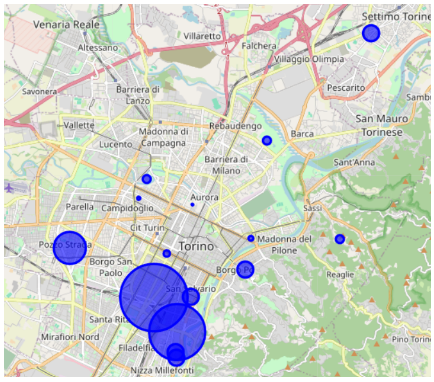

(b)

Figure 7 – Hospital needs of medicines in emergency scenario, in 2022. At the left the area shows the overall Piedmont region, at the right there is a zoom of Turin.

	eVTOL	*Drone*	*Car*
Merit Index	0.88	0	0.12

Table 5 – Results of analysis for Urgent delivery of "Kovaltry".

value from equation (10) has been considered for the Merit Index.

	eVTOL	Drone
Safety threshold	67 of 77	0 of 77
Payload threshold	77 of 77	3 of 77
Range threshold	60 of 77	34 of 77

Table 6 – Number of successfull deliveries with 2022 dataset - Urgent Priority

	eVTOL	Drone
Safety threshold	91 of 162	0 of 162
Payload threshold	159 of 162	3 of 162
Range threshold	112 of 162	71 of 162

Table 7 – Number of successfull deliveries in 2022 dataset - Medium Priority

	eVTOL	Drone
Safety threshold	129 of 256	0 of 256
Payload threshold	190 of 256	15 of 256
Range threshold	183 of 256	114 of 256

Table 8 – Number of successfull deliveries with 2022 dataset - Routine Priority

Table 9 shows the overall Index merit for eVTOL, drone and car, by averaging all the results.
The ideal position for eVTOL hub corresponds to an area between "Mauriziano" and "Città della Salute" hospitals, which are the healthcare facilities that needed more urgent deliveries in 2022 (Figure 9).
In Figure 10 we can see the position of the hub for ground transportation. Given the presence of road network, the ideal position is not in the center of Turin as for eVTOL but results in the outskirts.

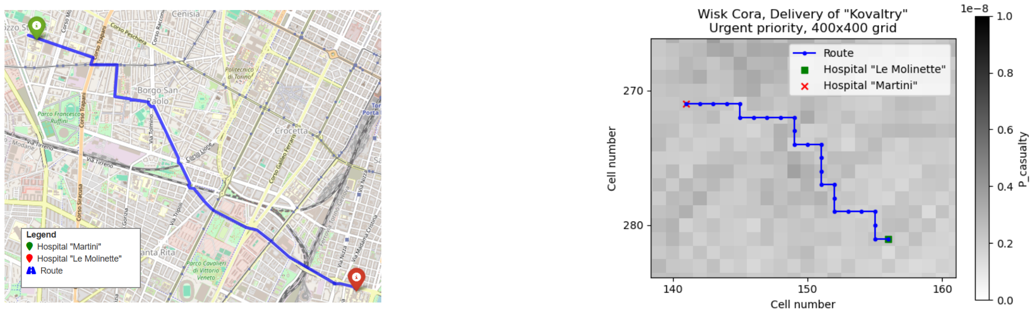

(a)

(b)

Figure 8 – Optimal path for Urgent delivery of "Kovaltry"; at the left ground transportation, at the right eVTOL over the risk map.

	eVTOL	Drone	Car
Urgent Priority	0.69	0	0.31
Medium Priority	0.42	0	0.58
Routine Priority	0.24	0	0.76

Table 9 – Average Merit Index for all deliveries in 2022

4. Discussion

Risk maps are valuable tools for path planning and evaluating the safety of routes. The maximum $P_{casualty}$ is in the order of magnitude of 10^{-8} for manned VTOLs and 10^{-2} for drones. In the calculation of $P_{casualty}$ in Equation (1), the value of P_{event} significantly influences the final result. Consequently, drone flights are nearly impossible from a safety perspective. The presence of sheltering from rooftops improves the situation; for example, in the latitudes 44.6° - 45.2° (corresponding to the city of Turin), the value is lower. However, overall, drone overflight is not acceptable for safety reasons. Therefore, although a risk map was not considered in this computation, we identify the no-fly zones in Italian cities for drones as currently regulated [33].

In the case of eVTOLs, although the effect of sheltering factor is negligible due to the high kinetic energy at impact, we find that flight is feasible on almost all routes. The A* algorithm suggests overflying non-populated areas when possibile, such as for Valle d'Aosta hospital, as shown in Figure 11. At the same time, the overall safety level is uder the threshold for eVTOL in most of paths, especially in short paths inside the city, altough they are on overcrowded zones. This finding confirms the feasibility of using eVTOLs in densely populated areas. From our analysis, it is crucial to carefully evaluate the design and construction philosophy of aircraft to ensure flight safety in crowded areas.

In priority scenarios, the most significant weight is assigned to delivery time, while cost is negligible, and safety has a weight of 5. As stated in Section 2.9, the compared values refer only to missions that satisfy all threshold requirements in cost, safety, and time. Consequently, this approach does not neglect safety; instead, it prioritizes the fastest means of transportation among those meeting all requirements.

Regarding the feasibility of deliveries, according to the historical data used in the analysis, VTOLs are the best means of transportation in urgent priority scenarios. This is demonstrated both in the single case of the "Kovaltry" delivery and in the overall data, with a merit index higher than that of cars, which are currently used for transportation. Specifically, for Kovaltry, the delivery time with VTOL is 433 seconds, compared to 811 seconds by car. The car's time corresponds to the value obtainable using Google Maps for the same route. Therefore, eVTOL stands out as the most suitable means of transportation for this single case. Extending the analysis to all urgent deliveries of 2022, this situation is confirmed, as the eVTOL has the highest merit index.

In medium-priority scenarios, where the cost weight is greater and the importance of time is lower, cars become more prioritized, though the difference is minimal (0.42 for VTOL versus 0.58 for cars).

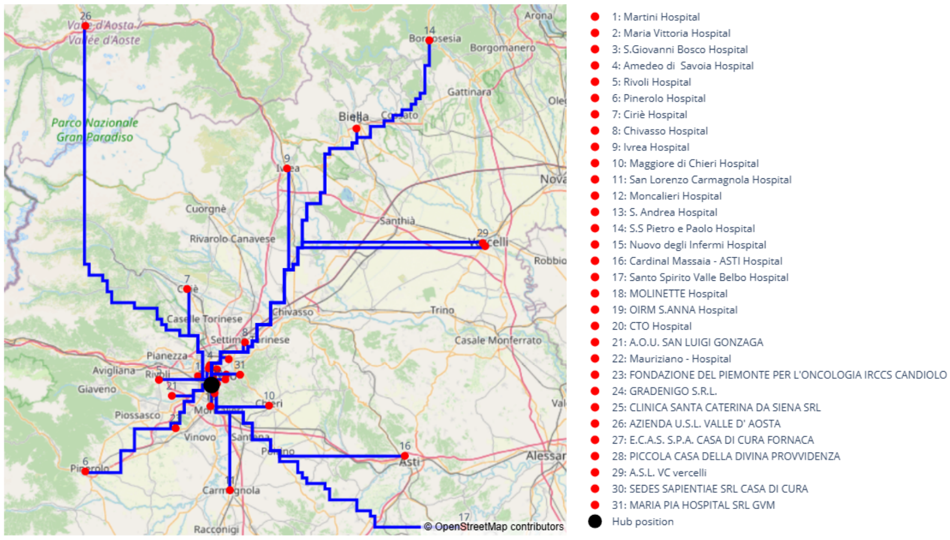

Figure 9 – Position of hub for eVTOL; it corresponds to an area between "Mauriziano" and "Città della Salute" hospitals.

From an economic perspective, the operational cost of VTOLs is approximately €87,000.00 for all deliveries in 2022, while the ground transportation cost is estimated at €14,000.00. Consequently, for routine scenarios, where cost and safety are significant factors, cars appear as the best means of transportation according to the merit index.
Determining the hub location can rationalize deliveries. The analysis of the optimal position for VTOLs shows that proximity to the most needy hospitals is the best strategy, as they have the most frequent needs. Our analysis indicates that the optimal location corresponds to a zone between "Mauriziano" and "Città della Salute" Hospitals; both facilities account for the majority of deliveries in the dataset. Similar results were found by Diaz et al. [7] regarding the proper hub location. Conversely, for ground transportation, the hub is best located outside the inner area of Turin due to road accessibility. In our model, the optimal location is near Cuorgné town, a finding consistent with an ongoing feasibility study by the Municipality of Turin [34].

5. Conclusion

This research has undertaken a comparative analysis of eVTOL, drone, and ground transportation systems for the emergency delivery of blood-derived medications. The findings offer valuable insights into the viability and efficiency of these transportation modes, particularly in densely populated urban areas such as Turin in Italy.
The study confirms that eVTOLs are the most suitable means of transportation for urgent priority scenarios. The merit index, which accounts for factors such as safety, delivery time, and cost, consistently favored eVTOLs over cars and drones. For example, in the case of the urgent delivery of the medication Kovaltry, the eVTOL completed the delivery in 433 seconds compared to 811 seconds by car. This trend was observed across all urgent deliveries analyzed for the year 2022, highlighting the quick response capability of eVTOLs, which is crucial for life-saving medications.
In medium-priority scenarios, the balance shifts slightly in favor of cars, primarily due to their lower operational costs and the reduced emphasis on delivery time. However, since the margin with the eVTOL is narrow, eVTOLs remain competitive.
For routine deliveries, where cost efficiency and safety are paramount, cars emerged as the most suitable means of transportation.
The study also explored the optimal placement of delivery hubs to maximize the efficiency of the

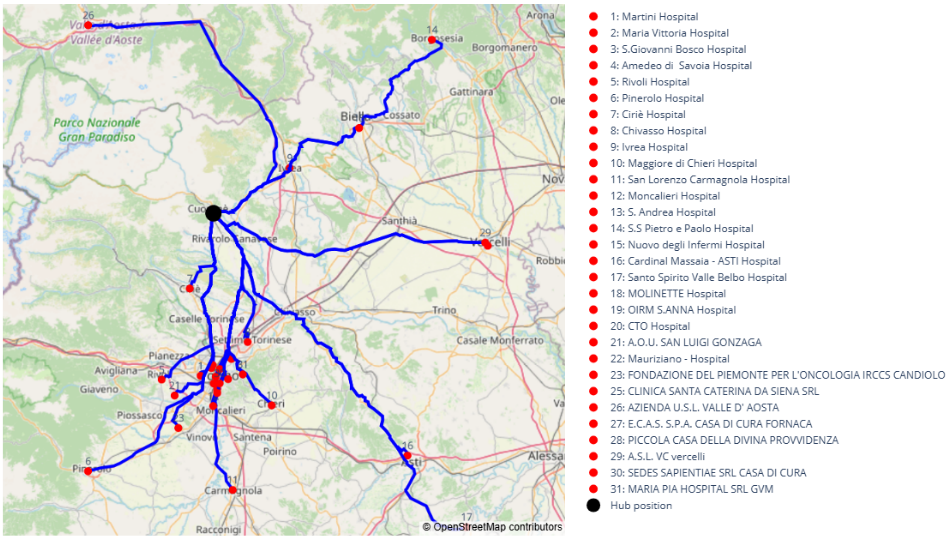

Figure 10 – Optimal hub position for ground transportation; it is outside Turin.

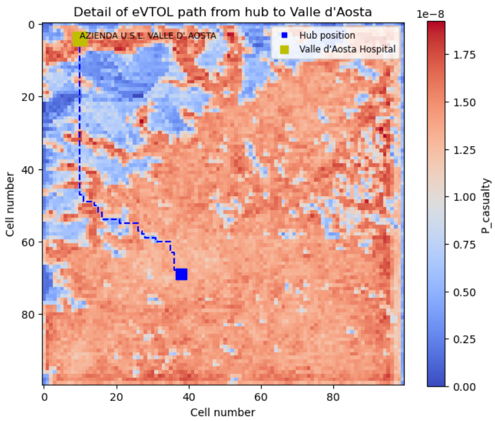

(a)

Data of the mission (round trip)	
Lenght of path (round trip) [km]	315
Average speed [minutes]	105
Overall risk $[h^{-1}]$	2.458 $\cdot 10^{-6}$

(b)

Figure 11 – Example of delivery from eVTOL hub to Valle d'Aosta Hospital, using a 100x100 grid on the urgent risk map.

transportation network. For eVTOLs, the analysis suggested that hubs should be located near hospitals with the highest demand for urgent medications. A point between "Mauriziano" and "Città della Salute" Hospitals, which had the greatest need for deliveries in 2022, was identified as the ideal hub location. This finding aligns with existing research and practical considerations, as proximity to high-demand areas reduces overall delivery times and enhances service reliability. For ground transportation, the optimal hub location was identified outside the inner area of Turin. This placement leverages the existing road network, thereby ensuring more efficient ground-based deliveries.
Overall, this study demonstrates that integrating eVTOLs into the emergency medical delivery infrastructure can significantly enhance response times and delivery efficiency, particularly for urgent medical needs. However, for routine deliveries, ground transportation remains the most cost-effective solution. Future research should continue to refine these models and explore additional factors more reliable drones, regulatory changes, and advancements in autonomous vehicle technologies to further optimize emergency medical logistics.

6. Contact Author Email Address

For future contacts: davide.angelini@polito.it; enrico.cestino@polito.it

This publication is part of the project PNRR-NGEU which has received funding from the MUR – DM 117/2023

Finanziato dall'Unione europea NextGenerationEU | Ministero dell'Università e della Ricerca | Italiadomani PIANO NAZIONALE DI RIPRESA E RESILIENZA

7. Copyright Statement

References

[1] Mohammad Moshref-Javadi, Matthias Winkenbach, “Applications and Research avenues for drone-based models in logistics: A classification and review", *Expert Systems with Applications*, Volume 177, 2021

[2] Lim JCL, Loh N, Lam HH, Lee JW, Liu N, Yeo JW, Ho AFW. The Role of Drones in Out-of-Hospital Cardiac Arrest: A Scoping Review. J Clin Med. 2022 Sep 28;11(19):5744.

[3] Kim, S.J., Lim, G.J., Cho, J. et al. Drone-Aided Healthcare Services for Patients with Chronic Diseases in Rural Areas. *J Intell Robot Syst.* 88, 163–180 (2017).

[4] Medical Drone Delivery Database, website; accessed 13th June 2024

[5] Oakey A, Grote M, Smith A, Cherrett T, Pilko A, Dickinson J, AitBihiOuali L. Integrating drones into NHS patient diagnostic logistics systems: Flight or fantasy? PLoS One. 2022 Dec 22;17(12):e0264669.

[6] Rosser JC Jr, Vignesh V, Terwilliger BA, Parker BC. Surgical and Medical Applications of Drones: A Comprehensive Review. JSLS. 2018 Jul-Sep;22(3):e2018.00018.

[7] Espejo-Díaz, J.A., Alfonso-Lizarazo, E. and Montoya-Torres, J.R. Improving access to emergency medical services using advanced air mobility vehicles. *Flex Serv Manuf J*, 2023

[8] De Filippis, L., Guglieri, G. and Quagliotti, F. Path Planning Strategies for UAVS in 3D Environments. *J Intell Robot Syst.*, 65, 247–264

[9] Deng, Zhao & Guo, Zhiming & Wu, Liaoni & You, Yancheng. “Trajectory Planning for Emergency Landing of VTOL Fixed-Wing Unmanned Aerial Vehicles". *Mobile Information Systems*. 2021

[10] Wisk Cora. *Introducing Generation 6*. Available: `https://wisk.aero/aircraft/`, Accessed 7 October 2023.

[11] Primatesta S, Rizzo A, Anders la Cour-Harbo. Ground Risk Map for Unmanned Aircraft in Urban Environments. *Journal of Intelligent & Robotic Systems*, Springer, 2019. Available: `https://doi.org/10.1007/s10846-019-01015-z`.

[12] Agenzia Italiana del Farmaco. *Farmaci emoderivati*. 2023. Available: `https://www.aifa.gov.it/emoderivati`, Accessed 18 September 2023.

[13] EDQM. *Guide to the preparation, use and quality assurance of Blood Components*. 21st edition, 2023.

[14] IFU of Kovaltry, from EMA website, Accessed 18 September 2023.

[15] EASA. *SPECIAL CONDITION Vertical Take-Off and Landing (VTOL) Aircraft*, Vol. SC-VTOL-01, Issue 1, 2019. Available: `https://www.easa.europa.eu/sites/default/files/dfu/SC-VTOL-01.pdf`.

[16] EASA. *Certification Specifications, Acceptable Means of Compliance and Guidance Material for Small Rotorcraft (CS-27)*, Vol. Amendment 10, 27 January 2023.

[17] EASA. *Certification Specifications and Acceptable Means of Compliance for Large Aeroplanes (CS-25)*, Vol. Amendment 27, 24 November 2021.

[18] Facebook Connectivity Lab and Center for International Earth Science Information Network - CIESIN - Columbia University. 2016. *High Resolution Settlement Layer (HRSL). Source imagery for HRSL © 2016 DigitalGlobe*. Available: `https://data.humdata.org/dataset/`

italy-high-resolution-population-density-maps-demographic-estimates, Accessed 10 December 2022.

[19] Doxsey-Whitfield E, MacManus K, Adamo SB, et al. Taking Advantage of the Improved Availability of Census Data: A First Look at the Gridded Population of the World, Version 4. *Papers in Applied Geography*, Vol. 1, pp. 226-234, 2015. Routledge. Available: https://doi.org/10.1080/23754931.2015.1014272.

[20] Federal Aviation Administration. *EXPECTED CASUALTY CALCULATIONS FOR COMMERCIAL SPACE LAUNCH AND REENTRY MISSIONS*, Vol. 431.35-1, 2020. Available: https://www.faa.gov/about/office_org/headquarters_offices/ast/licenses_permits/media/Ac4311fn.pdf.

[21] Bacchini A, Cestino E. Electric VTOL Configurations Comparison. *Aerospace*, 2020. DOI: https://doi.org/10.3390/aerospace6030026.

[22] Anders la Cour Harbo. Ground impact probability distribution for small unmanned aircraft in ballistic descent. 2020. DOI: 10.1109/ICUAS48674.2020.9213990.

[23] D. Angelini, "Progettazione e valutazione di un sistema di trasporto innovativo aereo per farmaci emoderivati in condizione di emergenza", *Politecnico di Torino*, 2023

[24] Dalamagkidis K, Valavanis KP, Piegl LA. *On Integrating Unmanned Aircraft Systems into the National Airspace System*. 2nd edition, Journal of Intelligent & Robotic Systems, Springer, 2012. DOI: 10.1007/978-94-007-2479-2.

[25] Range Safety Group, Range Commanders Council. *Common Risk Criteria standards for national test ranges: Supplement, Supplement to documento 321-027*, Vol. 88002-5110, Army White Sands Missile Range, 2007.

[26] Dijkstra, E.W., A note on two problems in connexion with graphs, *Numerische Mathematik*, 269–271 (1959).

[27] P. E. Hart, N. J. Nilsson and B. Raphael, "A Formal Basis for the Heuristic Determination of Minimum Cost Paths", *IEEE Transactions on Systems Science and Cybernetics*, vol. 4, no. 2, pp. 100-107, July 1968

[28] František Duchoň, Andrej Babinec, Martin Kajan, Peter Beňo, Martin Florek, Tomáš Fico, Ladislav Jurišica, "Path Planning with Modified a Star Algorithm for a Mobile Robot", *Procedia Engineering*, Volume 96, 2014, Pages 59-69

[29] Grande A. *L'INCIDENTALITA' STRADALE SULLA RETE VIARIA PRINCIPALE*, Ministero delle Infrastrutture e dei Trasporti, 2017. Available: https://www.certifico.com/component/attachments/download/7422.

[30] Aircraft Cost Calculator. *ROBINSON R44 Raven II*. Available: https://www.aircraftcostcalculator.com/AircraftOperatingCosts/531/Robinson+R44+Raven+II#:~:text=Based%20on%20450%20annual%20owner,down%20to%20%24475.00%20per%20hour., Accessed 9 October 2023.

[31] Duffy MJ, et al. A Study in Reducing the Cost of Vertical Flight with Electric Propulsion. *Aerospace*, 17th AIAA Aviation Technology, Integration, and Operations Conference, June 2017. DOI: http://dx.doi.org/10.2514/6.2017-3442.

[32] Cestino E, Romeo G. INNOVATIVE UNMANNED AIRCRAFTS: ROLE AND CONSTRAINTS FOR GMES APPLICATIONS. 3rd CEAS Air & Space Conference 21st AIDAA Congress 24, October 2011.

[33] ENAC. *Regolamento UAS-IT*. January 2021. Available: https://www.enac.gov.it/sites/default/files/allegati/2021-Gen/Regolamento_UAS-IT080121.pdf, Accessed 11 October 2023.

[34] LOSA, un progetto per creare un hub del farmaco in Canavese. 9-10 November 2017. Available: http://www.cittametropolitana.torino.it/cms/comunicati/attivita-produttive/losa-un-progetto-per-creare-un-hub-del-farmaco-in-canavese, Accessed 18 September 2023.